2nd URSI AT-RASC, Gran Canaria, 28 May – 1 June 2018

Ultra-Wideband Reconfigurable Filter with Electronically-Switchable Bandpass/Bandstop States

Chenyue Shi(1), Wenjie Feng(1), Roberto Gómez-García(2), Xiyan Zhang(1), Yumeng Zhang(1), and Wenquan Che(1)
(1) Department of Communication Engineering, Nanjing University of Science and Technology, Nanjing, 210094, China
(2) Department of Signal Theory and Communications, Polytechnic School, University of Alcalá, 28871 Madrid, Spain

Abstract

A novel multi-functional reconfigurable filter with four ultra-wideband (UWB) operational modes is presented. It consists of a transversal signal-interference filter structure with two controllable electrical paths, as follows: a main path made up of a commutable-open/short-ended quarter-wavelength coupled-line stage, and a secondary path with a selectable transmission line and short-ended stubs. In this manner, by switching these elements ON/OFF through p-i-n diodes, three bandpass-filter (BPF) and one bandstop-filter (BSF) states can be set. Moreover, the bandwidth for the sharp-rejection BPF states can be discretely controlled through the transmission zeros (TZs) created by the signal-interference effect and the stubs. For practical validation, a 1-GHz UWB microstrip prototype with bandwidths of 79.3%, 98.9% and 111.7% for the BPF modes and of 114.2% for the BSF mode is developed and characterized.

1. Introduction

Reconfigurable filters may play a key role in modern multi-mode and broad-band RF wireless systems (e.g., 5G) for commercial, civil, and defense applications. This is due to their capability to flexibly adapt their operation to different RF-signal conditions, as well as their lower size and DC-power consumption when compared to filter banks [1].

Among the years, a large plurality of frequency-adaptive RF filters in terms of center frequency, bandwidth, transmission zeros (TZs), and type of filtering profile have been reported [2-9]. Multi-functional filters usually refer to the last category, as those filtering components that feature both bandpass-filter (BPF) modes for dynamic RF-signal acquisition and bandstop-filter (BSF) modes for spectrally-agile interference suppression in the same circuit volume. Nevertheless, prior-art multi-functional RF filters, such as those reported in [7, 8], do not exhibit ultra-wideband (UWB) operation for all their selectable filtering states.

In this paper, a new type of multi-functional reconfigurable filter with UWB characteristics for its BPF and BSF states is presented. It is an evolved version of the switchable filter concept described in [9] to exhibit UWB operation for all its filtering modes, which are obtained from the controlled signal interference between its two transversal signal-propagation paths [10, 11]. Thus, through the interaction between a main path and a secondary transmission path with controllable characteristics through p-i-n switches, multiple BPF and BSF responses can be reconfigured. For experimental-validation purposes, a 1-GHz electronically-switchable microstrip prototype with three UWB BPF states and one UWB BSF state is manufactured and tested.

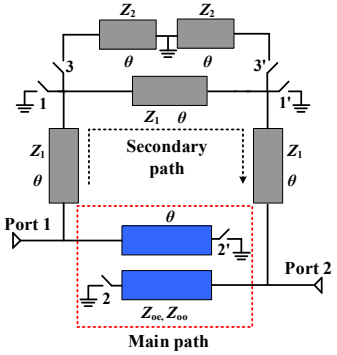

Figure 1. Circuit detail of the proposed UWB reconfigurable multi-functional filter concept.

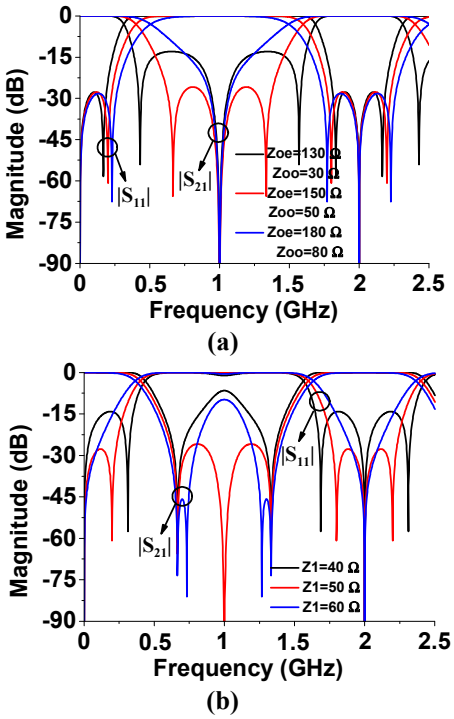

Figure 2. UWB-BSF mode. **(a)** Frequency responses $|S_{21}|$ and $|S_{11}|$ versus Z_{oe}, Z_{oo} (Z_1 = 50 Ω). **(b)** Frequency responses $|S_{21}|$ and $|S_{11}|$ versus Z_1 (Z_{oe} = 150 Ω, Z_{oo} = 50 Ω).

2. Theoretical Foundations

Fig. 1 shows the ideal-circuit detail of the engineered reconfigurable multi-functional filter concept. As can be seen, it consists of two switchable transmission paths (namely, main and secondary paths) that are connected in parallel. The main path is a quarter-wavelength coupled-line stage (Z_{oe}, Z_{oo}, θ) whose extremes can be switched between open- and short circuits, whereas the secondary path is made up of a three-quarter-wavelength transmission line (Z_1, 3θ) and two quarter-wavelength short-ended stubs (Z_2, θ). In this manner, by commutating ON/OFF the different circuit elements with a total of six switches (referred to as switches 1, 1', 2, 2', 3, 3' in Fig. 1), different filter schemes that result in three distinct UWB BPF and one UWB BSF transfer functions are produced. They are derived from constructive and destructive signal-interference effects for passband and stopband creation, respectively, among the two electrical paths of this reconfigurable multi-functional filtering architecture. The four operational modes and their setting for this filter concept are described below (center frequency f_0 = 1 GHz and reference impedance Z_0 = 50 Ω):

- UWB-BSF mode: all switches OFF. Thus, the main path is an open-ended quarter-wavelength coupled-line stage (Z_{oe}, Z_{oo}, θ) and the secondary path is a three-quarter-wavelength transmission line (Z_1, 3θ). Fig. 2 represents examples of the theoretical frequency responses of this filter mode as a function of Z_{oe}, Z_{oo} (Fig. 2(a)) and Z_1 (Fig. 2(b)). As proven, UWB BSF responses are generated in all cases, in which the stopband bandwidth increases as the coupling coefficient of the coupled-line stage and Z_1 get higher.
- UWB-BPF-1 mode: switches 1, 1' ON and the remaining ones OFF. In this manner, the resulting filter arrangement is an open-ended quarter-wavelength coupled-line stage (Z_{oe}, Z_{oo}, θ) with short-ended quarter-wavelength stubs (Z_2, θ) at its input and output accesses. As illustrated in Fig. 3 where example frequency responses are plotted, an UWB BPF behavior is obtained, whose passband-width is enlarged as the coupling coefficient, Z_1, and Z_2 are decreased. Note that the close-to-passband TZs are created by the short-ended stubs and give rise to sharp-rejection capabilities for all transfer functions. On the other hand, the TZs at DC and $2f_0$ are inherent to the coupled-line stage of the main path.
- UWB-BPF-2 mode: switches 2, 2' ON and the remaining ones OFF. In this case, the main path becomes a short-ended quarter-wavelength coupled-line stage (Z_{oe}, Z_{oo}, θ) and the secondary path a three-quarter-wavelength transmission line (Z_1, 3θ) with short-ended stubs. It results again in an UWB BPF behavior, in which the bandwidth is increased as the coupling coefficient of the main coupled-line path and Z_1 are increased (see Fig. 4).

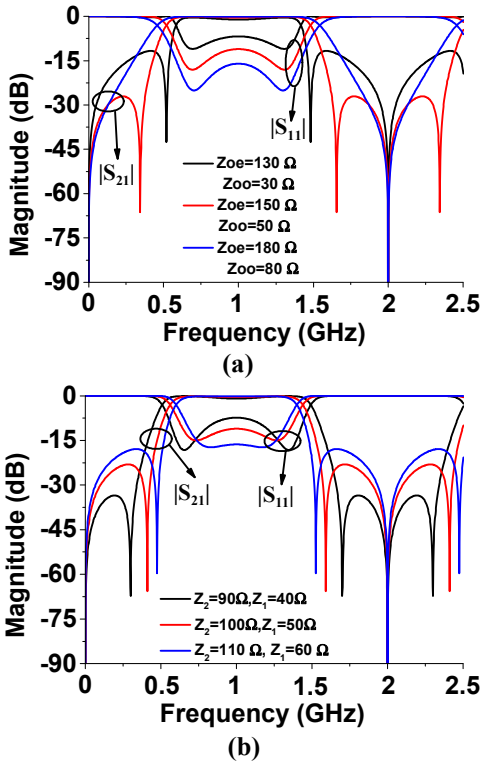

Figure 3. UWB-BPF-1 mode. **(a)** Frequency responses $|S_{21}|$ and $|S_{11}|$ versus Z_{oe}, Z_{oo} (Z_1= 50 Ω). **(b)** Frequency responses $|S_{21}|$ and $|S_{11}|$ versus Z_1 (Z_{oe} =150 Ω, Z_{oo} = 50 Ω).

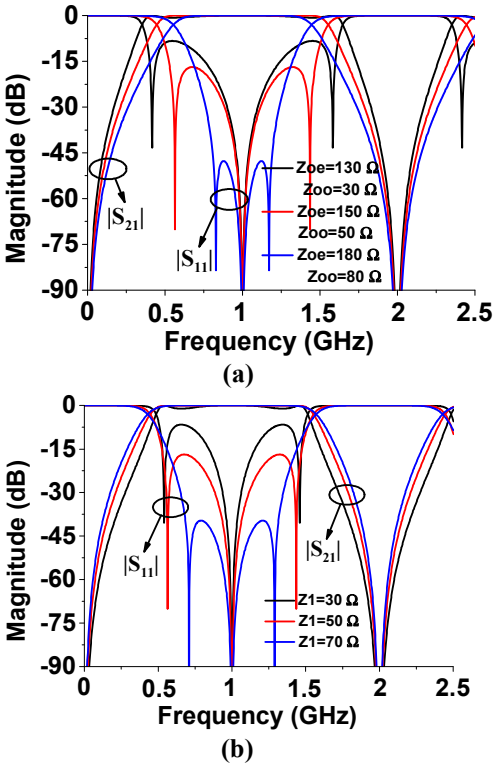

Figure 4. UWB-BPF-2 mode. **(a)** Frequency responses $|S_{21}|$ and $|S_{11}|$ versus Z_{oe}, Z_{oo} (Z_1= 50 Ω). **(b)** Frequency responses $|S_{21}|$ and $|S_{11}|$ versus Z_1 (Z_{oe} =150 Ω, Z_{oo} = 50 Ω).

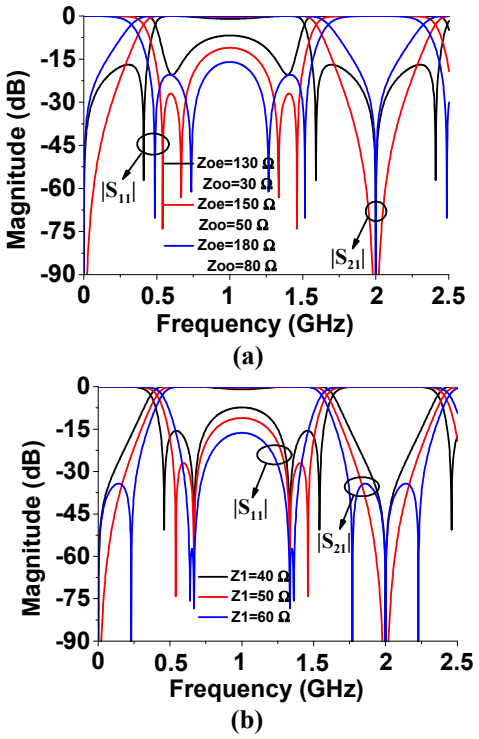

Figure 5. UWB-BPF-3 mode. **(a)** Frequency responses $|S_{21}|$ and $|S_{11}|$ versus Z_{oe}, Z_{oo} (Z_1 = 50 Ω, Z_2 = 100 Ω). **(b)** Frequency responses $|S_{21}|$ and $|S_{11}|$ versus Z_1 (Z_{oe} =150 Ω, Z_{oo} = 50 Ω, Z_2 = 100 Ω).

- UWB-BPF-3 mode: switches 1, 1' OFF and the remaining switches ON. Thus, the main path is a short-ended quarter-wavelength coupled-line stage (Z_{oe}, Z_{oo}, θ) and the secondary path is a three-quarter-wavelength transmission line (Z_1, 3θ). Like in the two previous cases, a UWB BPF operation is again set in which the bandwidth is broadened as the coupling coefficient in the main coupled-line path and Z_1 are reduced (see Fig. 5).

3. Experimental Results

For practical verification and based on the previous theoretical analysis, a 1-GHz electronically-switchable multi-functional microstrip filter prototype with four UWB transmission modes has been built and measured. Its ideal-circuit variables as detailed in Fig. 1 are as follows (Z_0 = 50 Ω): Z_{oe} =140 Ω, Z_{oo} = 50 Ω, Z_1 = 50 Ω, and Z_2 = 100 Ω.

The layout of the developed circuit is provided in Fig. 6. The main characteristics of the employed Tai Xin F4B microstrip substrate are as follows: relative permittivity ε_r = 2.65, dielectric substrate h = 1 mm, and dielectric loss tangent $tan(\delta_D)$ = 0.003. To enhance the isolation effect associated to switches 1 and 1' for OFF state, one more p-i-n diode was added at the middle of the transmission-line segment that connects these switches as shown in Fig. 6. The values of the blocking capacitors and bias resistors are C_{block} = 1000 pF and R_{bias} = 1 kΩ. For all switches, p-i-n diodes SMP1345-079LF from Skyworks were selected. The values for the dimensions in Fig. 6, in mm, are as follows: w_1 = 2.68, w_2 = 0.7, w_3 = 0.71, l_1 = 4.6, l_2 = 6.32, l_3 = 9.15, l_4 = 9.3, l_5 = 8.65, l_6 = 5.64, l_7 = 61.36, l_8 = 3.47, l_9 = 56, l_{10} = 14.29, l_{11} = 19.58, l_{12} = 9.29, and s_1= 0.15.

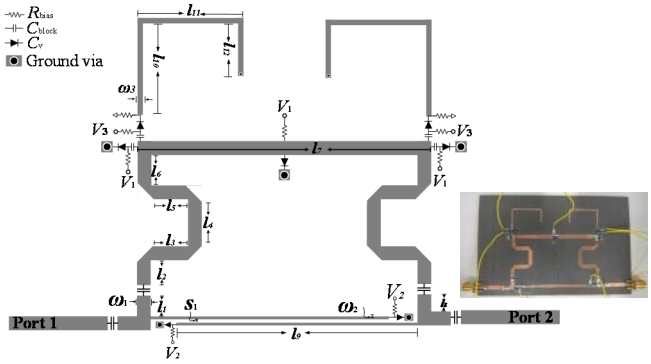

Figure 6. Manufactured 1-GHz electronically-switchable microstrip filter prototype (layout and photograph).

The measured and simulated power transmission, reflection, and group-delay responses for the four operational filtering modes are represented in Fig. 7. As can be seen, a fairly-close agreement between predicted and experimental results is attained so that the proposed UWB multi-functional filter concept is fairly verified. The main measured parameters for these states are as follows:

- UWB-BSF state (Fig. 7(a)): 3-dB fractional bandwidth of 114.2%, minimum in-band power-insertion loss of 9.4 dB, and group delay in passband ranges lower than 2 ns.
- UWB-BPF-1 state (Fig. 7(b)): 3-dB fractional bandwidth of 79.3%, minimum in-band power-return loss of 12.3 dB, and minimum in-band power-insertion loss of 1.47 dB, and in-band group delay below 2 ns.
- UWB-BPF-2 state (Fig. 7(c)): 3-dB fractional bandwidth equal to 98.9%, minimum in-band power-return loss of 14.1 dB, minimum in-band power-insertion loss of 0.93 dB, and in-band group delay lower than 2.5 ns.
- UWB-BPF-3 state (Fig. 7(d)): 3-dB fractional bandwidth equal to 111.7%, minimum in-band power-return loss of 12.1 dB, minimum in-band power-insertion loss of 1.3 dB, and in-band group-delay variation below 1.8 ns.

The IIP3 was measured for the UWB-BPF-3 state, which is between 30 dBm and 39 dBm in the range 2-4.5 GHz.

5. Conclusion

A new type of reconfigurable multi-functional filter with based on transversal signal-interaction concepts has been reported. It features three UWB BPF and one UWB BPF

modes that are obtained from constructive/destructive signal-combinations effects between the two switchable electrical paths of the structure. As experimental proof-of-concept, a microstrip prototype with electronic control through p-i-n diodes has been fabricated and tested. It is believed that this UWB switchable filter concept shows potential for future broad-band communication systems.

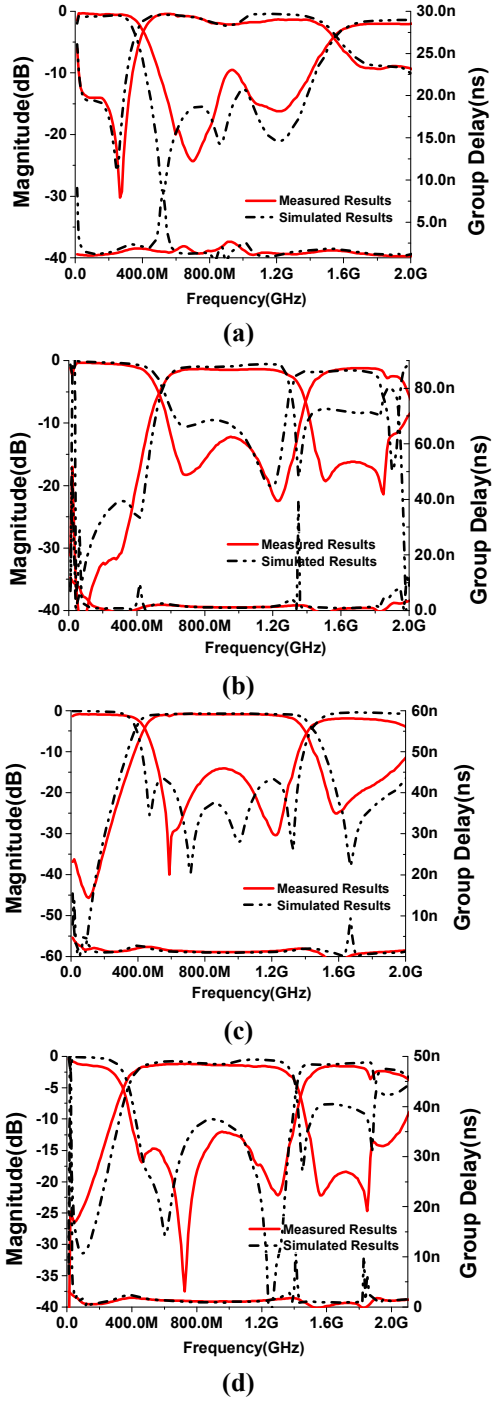

Figure 7. Simulated and measured power transmission, reflection, and group-delay responses of the manufactured 1-GHz electronically-switchable microstrip filter prototype **(a)** UWB-BSF mode. **(b)** UWB-BPF-1 mode. **(c)** UWB-BPF-2 mode. **(d)** UWB-BPF-3 mode.

5. References

1. W. J. Chappell, E. J. Naglich, C. Maxey, and A. C. Guyette, "Putting the radio in "Software-defined radio": Hardware developments for adaptable RF systems," *Proc. IEEE*, **102**, 3, Mar. 2014, pp. 307-320, doi: 10.1109/JPROC.2014.2298491.

2. I. Hunter and J. Rhodes, "Electronically tunable microwave bandpass filters," *IEEE Trans. Microw. Theory Techn.*, **30**, 9, Sep. 1980, pp. 1354-1360, doi: 10.1109/TMTT.1982.1131260.

3. H. Zhu and A. Abbosh, "Tunable band-pass filter with wide stopband and high selectivity using centre-loaded coupled structure," *IET Microw. Antennas Propag.*, **9**, 13, Sep. 2015, pp. 1371-1375, doi: 10.1049/iet-map.2014.0770.

4. W. Tu, "Compact low-loss reconfigurable bandpass filter with switchable bandwidth," *IEEE Microw. Wirel. Compon. Lett.*, **20**, 4, Apr. 2010, pp. 208-210, doi: 10.1109/LMWC.2010.2042553.

5. A. Miller and J.-S. Hong, "Wideband bandpass filter with reconfigurable bandwidth," *IEEE Microw. Wirel. Compon. Lett.*, **20**, 12, Dec. 2010, pp. 28-30, doi: 10.1109/LMWC.2017.2746679.

6. R. Gómez-García, M.-Á. Sánchez-Soriano, K. W. Tam, and Q. Xue, "Flexible filters: reconfigurable-bandwidth bandpass planar filters with ultra-large tuning ratio," *IEEE Microw. Mag.*, **15**, 5, Jul./Aug. 2014, pp. 43-54, doi: 10.1109/MMM.2014.2321094.

7. T. Yang and G. M. Rebeiz, "Bandpass-to-bandstop reconfigurable tunable filters with frequency and bandwidth controls," *IEEE Trans. Microw. Theory Techn.*, **65**, 7, Jul. 2017, pp. 2288-2297, doi: 10.1109/TMTT.2017.2679182.

8. D. Psychogiou, R. Gómez-García, and D. Peroulis, "Fully-reconfigurable bandpass/bandstop filters and their coupling-matrix representation," *IEEE Microw. Wireless Compon. Lett.*, **26**, 1, Jan. 2016, pp. 22-24, doi: 10.1109/LMWC.2015.2505635.

9. W. Feng, Y. Shang, W. Che, R. Gómez-García, and Q. Xue, "Multi-functional reconfigurable filter using transversal signal-interaction concepts," *IEEE Microw. Wireless Compon. Lett.*, **27**, 11, Nov. 2017, pp. 980-982, doi: 10.1109/LMWC.2017.2750022.

10. R. Gómez-García and J. I. Alonso, "Design of sharp-rejection and low-loss wideband planar filters using signal-interference techniques," *IEEE Microw. Wireless Compon. Lett.*, **15**, 8, Aug. 2005, pp. 530-532, doi: 10.1109/LMWC.2005.852797.

11. W. J. Feng, W. Q. Che, and Q. Xue, "Transversal signal interaction: Overview of high-performance wideband bandpass filters", *IEEE Microw. Mag.*, **15**, 2, Mar. 2014, pp. 84-96, doi: 10.1109/MMM.2013.2296216.